European Journal of Cardio-Thoracic Surgery 53 (2018) 512–518
doi:10.1093/ejcts/ezx352 Advance Access publication 27 September 2017

REVIEW

Cite this article as: Okusanya OT, Hess NR, Luketich JD, Sarkaria IS. Infrared intraoperative fluorescence imaging using indocyanine green in thoracic surgery. Eur J Cardiothorac Surg 2018;53:512–8.

Infrared intraoperative fluorescence imaging using indocyanine green in thoracic surgery

Olugbenga T. Okusanya*, Nicholas R. Hess, James D. Luketich and Inderpal S. Sarkaria

Department of Cardiothoracic Surgery, University of Pittsburgh Medical Center, Pittsburgh, PA, USA

* Corresponding author. Department of Cardiothoracic Surgery, University of Pittsburgh Medical Center, 200 Lothrop Street, Pittsburgh, PA 15213, USA. Tel: +1-215-5198170; e-mail: okusanyaot@upmc.edu (O.T. Okusanya).

Received 21 June 2017; received in revised form 15 August 2017; accepted 30 August 2017

Summary

Thoracic surgery faces many unique challenges that require innovative solutions. The increase in utilization of minimally invasive practices, poor overall cancer survival and significant morbidity of key operations remain key obstacles to overcome. Intraoperative fluorescence imaging is a process by which fluorescent dyes and imaging systems are used as adjuncts for surgeons in the operating room. Other surgical subspecialists have shown that intraoperative fluorescence imaging can be applied as a practical adjunct to their practices. Thoracic surgeons over the last 15 years have also used intraoperative fluorescence imaging for sentinel lymph node mapping, lung mapping, oesophageal conduit vascular perfusion and lung nodule identification. This review describes some of the key studies that demonstrate the applications of intraoperative near-infrared fluorescence imaging.

Keywords: Imaging • Oesophageal cancer • Segmentectomy • Lung cancer surgery • Sentinel lymph nodes • Indocyanine green

INTRODUCTION

Thoracic surgery is a constantly evolving field that continues to face important challenges such as the persistently high mortality from lung cancer and the high morbidity of oesophageal surgery. Thoracic surgeons must maintain a sense of versatility and innovation to adapt to ever evolving diseases, treatment strategies and technological innovation. One continuing focus is achieving maximal therapeutic benefit offered through surgical intervention while minimizing procedure-related morbidity. Over the last few decades, minimally invasive operative approaches have aimed to reduce surgical morbidity and potentially increase the proportion of patients that may tolerate and benefit from surgery. The advent of video-assisted thoracoscopic surgery, robotic surgery, lung volume reduction surgery and minimally invasive oesophagectomy represent just a few of many recent advances surgeons have made over the last century. It is likely that novel intraoperative imaging technologies may represent one of the next major advances in the surgical care of these patients.

Intraoperative fluorescence imaging (IFI) is the utilization of a fluorescence-emitting contrast agent and imaging system to enhance the surgeon's ability to perform an operation. IFI requires a unique interface of a disease model, tracer and intraoperative fluorescence imaging device (IFID). IFI has shown a number of applications with varying levels of success [1–3]. IFI has shown utility in identification of sentinel lymph nodes (SLNs) in several cancers, including breast cancer, melanoma, gastric cancer, prostate cancer and colon cancer [4–7]. IFI has also been used to identify and help clear metastatic tumour in ovarian and colon cancers [3, 8]. In thoracic surgery, the applications of IFI have been focused on sentinel lymph node biopsy (SLNB), lung mapping for pulmonary resection, vascular assessments of gastric conduits and for the localization of pulmonary nodules. Almost all of these studies have been performed using indocyanine green (ICG) as the sole Food and Drug Administration (FDA)-approved fluorescent contrast agent of choice. In this review, we focus on summarizing the current applications and uses of ICG-guided IFI in the field of thoracic surgery.

METHODS

A search of PubMed was conducted using iterations of the phrases 'indocyanine green', 'thoracic', 'surgery', 'ICG', 'intraoperative', 'fluorescence' and 'imaging' to locate any studies describing thoracic IFI in humans. These studies were then reviewed and categorized (Table 1).

INDOCYANINE GREEN

ICG is a water-soluble anionic, amphiphilic infrared fluorophore with a molecular weight of 774.9 kDA [9]. When given systemically, ICG binds rapidly in the vascular compartment to plasma proteins and lipoprotein, forming a nanoparticle [9]. The liver uptakes and excretes greater than 80% of available ICG into bile within 18 h [9]. ICG is safe at systemic doses as high as 5 mg/kg, though limited cases of anaphylaxis have been reported. ICG is

Table 1: Published studies using ICG as an intraoperative near-infrared imaging agent for thoracic surgery

Published human studies on near-infrared intraoperative fluorescence imaging in thoracic surgery by topic ($n > 5$)

	Study	Year	Dose	Route	Number of cases	Success (%)	Anastomotic leak (%)
Sentinel lymph node biopsy	Lung						
	Ito	2004	25 mg	Peritumoural	38	87.5	
	Yamashita	2011	10 mg	Peritumoural	61	80.3	
	Yamashita	2012	10 mg	Peritumoural	31	80.7	
	Colson	2013	3.8–2500 μg	Peritumoural	38	89	
	Nomori	2016	10 mg	Peritumoural	135	84	
Oesophagus							
	Yuasa	2012	0.5 ml (0.5%)	Peritumoural (transmural)	20	90	
	Hatchey	2016	2.5 mg	Peritumoural (endoscopic)	9	66	
Lung mapping							
	Misaki	2010	3 mg/kg	Systemic	8	100	
	Kasai	2013	3 mg/kg and 0.5 mg/kg	Systemic	30	93	
	Sekine	2012	30 ml	Intrabronchial	10	100	
	Tarumi	2014	3 mg/kg	Systemic	31	90	
	Lizuka	2016	5 mg/kg	Systemic	73	98	
Vascular perfusion							
	Kubota	2013	0.5 mg/kg	Systemic	5	80	0
	Rino	2014	2.5 mg	Systemic	33	100	15
	Shimada	2011	2.5 mg	Systemic	33	100	10
	Campbell	2015	5 mg	Systemic	30	100	0
	Koyanagi	2016	2.5 mg or 1.25 mg	Systemic	40	100	17.5
Tumour detection							
	Singhal	2014	5 mg/kg	Systemic	18	91	
	Kim	2016	1 mg/kg	Systemic	11	91	
	Yasafuku	2017	0.00125 mg	Transthoracic	20	90	
	Abbass	2017	5–10 mg	ENB	30	98	
	Hatchey	2017	1.2–2.5 mg	ENB	12	100	

Studies were included if they had greater than 5 patients and fell into the above subcategories. Success was defined as the ability to detect fluorescent signal discernible from background from the target tissue.
ENB: electromagnetic navigational bronchoscopy; ICG: indocyanine green.

the most intensively studied near-infrared (NIR) contrast agent and was approved by the US FDA for human administration in 1958. ICG is a cyanine fluorophore with a peak absorption wavelength of 778 nm and 805 nm when dissolved in water and plasma, respectively. The NIR emission spectra of ICG in plasma (830 nm) allow for tissue penetration of up to 10–15 mm and avoid autofluorescence from endogenous tissues [10]. Also, the protein binding of ICG has been shown to increase the spectral intensity, making it an excellent agent for *in vivo* analysis [10]. The amphiphilic attributes and protein-binding properties allow ICG to migrate within lymphatic channels. In addition, ICG is cheap, non-toxic and readily available, making it an ideal contrast agent for IFI. However, the uses of ICG in these studies are experimental, as the FDA specifically approves ICG for cardiac output, hepatic function and ophthalmic angiography.

SENTINEL LYMPH NODE BIOPSY

An SLN is the first draining lymph node from an anatomical location of a cancer, and the pathological status of this lymph node accurately predicts lymphatic metastatic cancer spread and greatly affects overall prognosis [11–13]. SLN mapping remains an intense area of interest for thoracic surgeons. For early-stage lung cancers, 5-year survival rate remains low at 73% with a high incidence of recurrence [14–16]. It is believed that these findings are in part due to occult lymph nodal disease not identified with current staging modalities, leading to initial understaging of these cancers [17, 18]. Prior attempts using non-fluorescent tracers for lung cancer SLNB have found limited success [19, 20]. Currently, mediastinoscopy and endobronchial ultrasound with biopsy remain the mainstays of preoperative mediastinal assessment, whereas systematic lymph node sampling or dissection at the time of surgery is the mainstay of intraoperative assessment. Mediastinoscopy is the direct biopsy of mediastinal lymph nodes using a telescope via a transcervical incision, and endobronchial ultrasound is the use of ultrasound-equipped bronchoscopy to perform fine needle aspiration of mediastinal lymph nodes. Systematic lymph node sampling requires the analysis of at least one lymph node from the surgically accessible mediastinal lymph node stations while dissection requires the removal of all mediastinal lymphatic tissue in the surgical field. Technologies aimed at improving nodal assessment may help decrease the rates of stage migration.

The first published studies of ICG as a SLN tracer for lung cancer was reported in 2004 [21]. Thirty-eight patients undergoing thoracotomy for pulmonary resection had 25 mg of ICG and 400 U of hyaluronidase injected directly into the peritumoural area. The pulmonary resection was immediately performed and followed by the lymphadenectomy. *Ex vivo*, the lymph nodes from the mediastinal lymphadenectomy were then visually inspected for ICG and then digested and analysed by spectrometry

to detect ICG. This group defined an SLN as any lymph node having an ICG concentration 1.25 times greater than the mean of all lymph nodes, which is not a known standard for SLN definition. This technique identified SLNs in every case as mandated by the methodology. The status of the SNL had a 97% predictive value for the status of all lymph nodes and a sensitivity of 87.5%. In 1 patient, the paratracheal Station 4 lymph node was determined to be the SLN by their definition, but the patient had metastatic disease in Stations 12 and 13 nodal basins. In this scenario, an N2 lymph node basin more distal to the tumour was determined to be the SLN basin, but the more proximal lymph nodes (N1) contained tumour. This patient was classified as having a false-negative SLN. Designating the SNL to be the node with an arbitrary concentration of ICG is questionable and lacks supporting data. Also, this technique required digestion of the lymph node, which may destroy positive tumour deposits within the digested tissue.

Two studies by Yamashita *et al.* [22, 23] in 2011 and 2012 used a minimally invasive, non-destructive IFI approach to human lung SNL identification with ICG. In 61 patients, 10 mg of ICG was injected into the peritumoural area. The lung was serially inflated and deflated, and after 10 min, the lymph nodes were inspected in real time using a minimally invasive IFID. This approach yielded a lower rate of SLN detection (80.3%). Failures were attributed to mechanical issues, such as adhesions and incomplete fissures. Their false-negative rate was comparable to the 2004 study at 2.1% [22, 23]. The difference in detection maybe related to the real-time inspection rather than the *ex vivo* arbitrary spectroscopic analysis.

A promising study on ICG as a lung SLN tracer was a dose escalation trial in humans [24]. ICG doses of 3.8 μg to 2500 μg were dissolved in human serum albumin or fresh-frozen plasma and injected into the peritumoural lung tissue of 38 patients undergoing pulmonary resection. The lung was inflated for 10 min to improve lymphatic circulation and either an open system IFID or a minimally invasive IFID was used to inspect the lymph node basins. Their results showed that SLN detection was a dose-dependent phenomenon. If less than 600 μg of ICG was injected, only 25% of the SLNs were detected, whereas if 1000 μg or greater was injected, the detection rate increased to 89%. Notably at 2500 μg ($n = 4$), 100% of SNLs were detected. In the 26 patients where an SLN was identified, the false-negative rate was 0%. Interestingly, 27% of patients had SLNs that were at a N2 location confirming the potential for 'skip' metastasis. Skip metastasis is the phenomenon in lung cancer of N2 (mediastinal) lymph node basins being positive for cancer while N1 (Hilar and more distal) basins are negative. However, this study did not identify any SLNs that were concurrently in the N2 station and also positive for metastatic disease. Despite this, the study strongly suggests that IFI NIR is a viable and an accurate technique for identification of SLNs, even in the face of the 'skip' metastasis phenomenon in lung cancer.

A recent study by Nomori *et al.* [25] used locally injected ICG (10 mg) for SLNB in early-stage lung cancers (T1N0M) during segmentectomy in relatively large series of patients ($n = 135$). They were successfully able to find lymph nodes in 84% of the cases. Fourteen of the patients had pathologically positive lymph nodes and 11 of these patients were located by IFI. The false-negative rate in this study was significant, though they were able to detect skip N2 lesions. Overall, IFI SNLB in lung cancer may be a promising technique to identify the lymph node packet that will predict overall nodal status. However, there is a lack of evidence that skip N2 lesions can be accurately or reliably detected. Secondly, the overall rate of detection of any SLN is still variable and not currently ready for broadscale clinical application.

SLNB using IFI has been applied to the treatment of oesophageal cancer. Yuasa *et al.* [26] were the first to show in 2012 that direct external injection of ICG in the peritumoural area of the oesophagus clearly demonstrated the lymphatic channels around the tumour. Twenty patients underwent a thoracotomy and had 0.5 mg of ICG injected directly into the submucosa around the tumour. NIR signal was then detected from the tissues surrounding the oesophagus, and these lymph nodes were harvested. These were all considered SLNs. In this study, they identified an SLN in 19 of 20 (95%) patients but had a 25% (1 of 4) false-negative rate.

Hachey *et al.* [27] conducted a study looking at the safety and feasibility of endoscopic ICG delivery for lymph node mapping rather than specifically for SNLB. They enrolled 10 patients with oesophageal adenocarcinoma who were scheduled for oesophagectomy. Each had 2.5 mg of ICG dissolved in 1 cm^3 of sterile water or 25% albumin alone was injected into the submucosa around the tumour via endoscopy. Patients then underwent oesophagectomy with NIR imaging. One of the original 10 patients was excluded after the discovery of metastatic disease. They were able to detect a draining lymph node in 6 of 9 patients who underwent imaging. The 3 patients in whom no draining IFI-positive lymph node was detected were those in whom water was used rather than albumin. The pathological status of the NIR-positive lymph node was consistent with those of the other lymph nodes in the specimen as all were negative. In this work, high NIR signal near the tumour injection site limited the examination of some of the local lymph nodes. Two groups have also recently shown that endoscopic submucosal injection of ICG before oesophagectomy is capable of producing an NIR lymphatic map [28, 29]. In both of these studies, all patients were able to have NIR-positive lymph nodes detected. However, in the study by Helminen *et al.* [29], only 9 of total 19 positive lymph nodes were NIR positive, and in 2 of the 6 patients, positive lymph nodes were found in distant lymph nodes rather than the closest draining bin.

LUNG MAPPING

Pulmonary segmentectomy may be a reasonable alternative to lobectomy in early-stage lung cancers [30, 31]. A segmentectomy can be a more technically challenging operation than a lobectomy, as it requires a higher level of dissection into the lung parenchyma and requires correct identification and isolation of specific segmental vascular and bronchial anatomy. Additionally, another major technical challenge associated with segmentectomy is clear delineation of intersegmental parenchymal planes. Currently, surgeons may rely on a number of mechanisms to determine this plane. Examples include bronchial isolation and inflation, dye injection of the cut bronchial stump or simple estimation [32, 33]. Accurately finding these planes prevents the retention of devascularized tissue and also allows the surgeon to maximize surgical margins by clearing of potentially tumour harbouring draining lymphatic pathways. As such, surgeons have sought to utilize IFI to enhance their ability to intraoperatively determine these planes.

Misaki *et al.* [34] were among the first to apply ICG IFI to 8 humans undergoing segmental pulmonary resection. The

dominant artery to the planned segment for removal was first ligated, and then 3 mg/kg of ICG was injected systemically. The mean time to detection of demarcation was 13 s, and peak demarcation was observed after 28 s. They noted some difficulty with large tumours or in emphysematous lungs. However, clear demarcation was noted in all patients, and no morbidity was attributed to the use of this technique. In 2013, this same group compared using 1 or 2 wavelengths of light to determine the parenchymal differentiation and found similar results [35]. Other groups have shown that transbronchial instillation of a dilute ICG solution is also capable of demarcating the intersegmental plane [36]. The advantage of this approach was that a systemic dose of ICG was not necessary and did not require previous ligation of any vasculature. However, some staining of adjacent segments was noted using this technique, highly limiting its utility.

VASCULAR PERFUSION

Oesophagectomy remains the mainstay of treatment for oesophageal cancer, and anastomotic leaks represent a major contribution to morbidity and mortality of the procedure, with some centres reporting rates as high as 27% [37–40]. Adequate vascular perfusion of the neo conduit presents a key component in avoiding this morbidity [41–43]. Poor perfusion of the anastomosis has been associated with an increased leak rate, and several investigators have looked at improving blood flow or tolerance of ischaemia [44–46]. Theoretically, accurate assessment of perfusion in the intraoperative setting may help avoid creation of the anastomosis in areas of greater relative ischaemia, potentially reducing the incidence of postoperative anastomotic leak and its associated morbidity.

The simplest investigations of blood flow to conduits were performed using a bolus dose of 0.5 mg/kg with immediate observation of the conduit to subjectively observe for obvious areas of poor perfusion [47]. An observational study showed that in all ($n = 33$) patients, systemic injection of 2.5 mg of ICG would allow for visualization of the vascular supply to the conduit providing further proof of concept [48]. A study of 33 patients undergoing oesophagectomy and utilization of an intestinal conduit changed the operative course based on intraoperative ICG angiography. This study used a 2.5-mg bolus of ICG and immediate inspection of the conduit [49]. If poor ICG filling was noted, the conduit was 'super charged' by adding an arterial anastomosis. If poor ICG clearance was noted then additional venous drainage was added. Secondly, microvascular ICG penetration into the conduit was also observed. When microvascular ICG penetration was observed, no anastomotic leakage occurred in this study. However, in 1 patient with additional anastomosis performed for macroscopic ICG flow deficit, anastomotic leakage did occur. The authors asserted that overall, the ICG-driven additional anastomosis did decrease the overall leak rate though no statistical significance was shown.

In a promising study by Campbell *et al.* [43], the routine use of ICG IFI was used in addition to Doppler examination of the gastric conduit. A mark was placed at the last notable Doppler signal and at the area of ICG perfusion that was 75% as intense as the gastric antrum. The intrathoracic anastomosis was created between these 2 marks using a circular stapler. In the 60 patients prior to initiation of this protocol, the leak rate was 20%. However, in the subsequent 30 patients, where IFI was employed, the anastomotic leak rate was 0%. In this series, anastomotic leak was defined as amylase-rich fluid in the perianastomotic drain and clinical signs of a leak, either radiological evidence via barium swallow or the presence of a right empyema on computed tomography (CT) scan.

In another study by Koyanagi *et al.* [50], a 2.5-mg dose of ICG was given after gastric tube formation in 40 patients undergoing oesophagectomy. Two groups were then identified: those in whom the ICG fluorescence was detected simultaneously in the gastric conduit and in the vascular arcade at the point distal to the terminal pulsation of the right gastroepiploic artery and those in whom conduit perfusion lagged behind the vascular arcade. In the group with simultaneous perfusion of ICG in the conduit and the vascular arcade, there were 0 anastomotic leaks and in the groups with delayed filling there were 7 leaks (47%). In further analysis, it was determined that ICG flow less than 1.76 cm/s^2 had a 36.5 odds ratio of anastomotic leak with a confidence interval of 4–905.

NODULE DETECTION

The pulmonary nodule remains a diagnostic and therapeutic challenge for thoracic surgeons. With the widespread availability and higher resolution of modern CT, detection of smaller and less distinct nodules is increasingly common. Furthermore, as the US Preventative Service Task Force has recently issued recommendations of CT imaging screening for lung cancer in patients with significant smoking history, it is likely that surgeons will be faced with this clinical scenario more frequently [51]. Small nodules or nodules in difficult anatomical locations can present a significant challenge to accurately identify and localize intraoperatively, particularly if a minimally invasive approach is maintained. Also, the presence of additional occult malignant nodules not identified preoperatively but identified at the time of operation is not uncommon [52]. As such, a significant area of IFI investigation has been in the intraoperative identification and localization of pulmonary nodules.

ICG has been used for local injection to mark small tumours for resection. Ujiie and Yasafuke [53] demonstrated a technique for injecting 100–150 µl of 0.125 mg/ml ICG into 20 peripheral lung nodules under CT guidance at the time of microcoil deployment. Eighteen of the 20 (90%) nodules were localized solely by the use of a video-assisted thoracoscopic surgery NIR thoracoscope (Fig. 1). One nodule that was unable to be located was 4.8 cm from the lung surface, and in the other undetected nodule, there was a technical issue with the delivery of the ICG. Tumour size ranged from 0.5 cm to 2.4 cm. Abbas *et al.* [54] approached local injection of ICG for tumour detection using navigational bronchoscopy. Thirty patients with previously undiagnosed nodules underwent electromagnetic navigational bronchoscopy with peritumoural injection of 1–2 ml of ICG (5 mg/ml). Patients then underwent surgical resection. The overall success rate was reported as 98%. Tumour size ranged from 4 mm to 44 mm, with a mean depth from the pleura of 22 mm. There were no postoperative deaths. Both of these studies showed promise for the ability to label very small tumours and considerable depth from the pleural surface. Both authors alluded to dye injection techniques to enhance their ability to detect the ICG on the tumour surface.

Hachey *et al.* [55] recently published a new study combining tumour localization with SLNB. In their pilot study, 12 patients with suspected early lung cancers had navigational bronchoscopy performed with peritumoural injection of 0.5–1 ml of 2.5 mg/ml ICG dissolved in 25% human serum albumin. The patients then

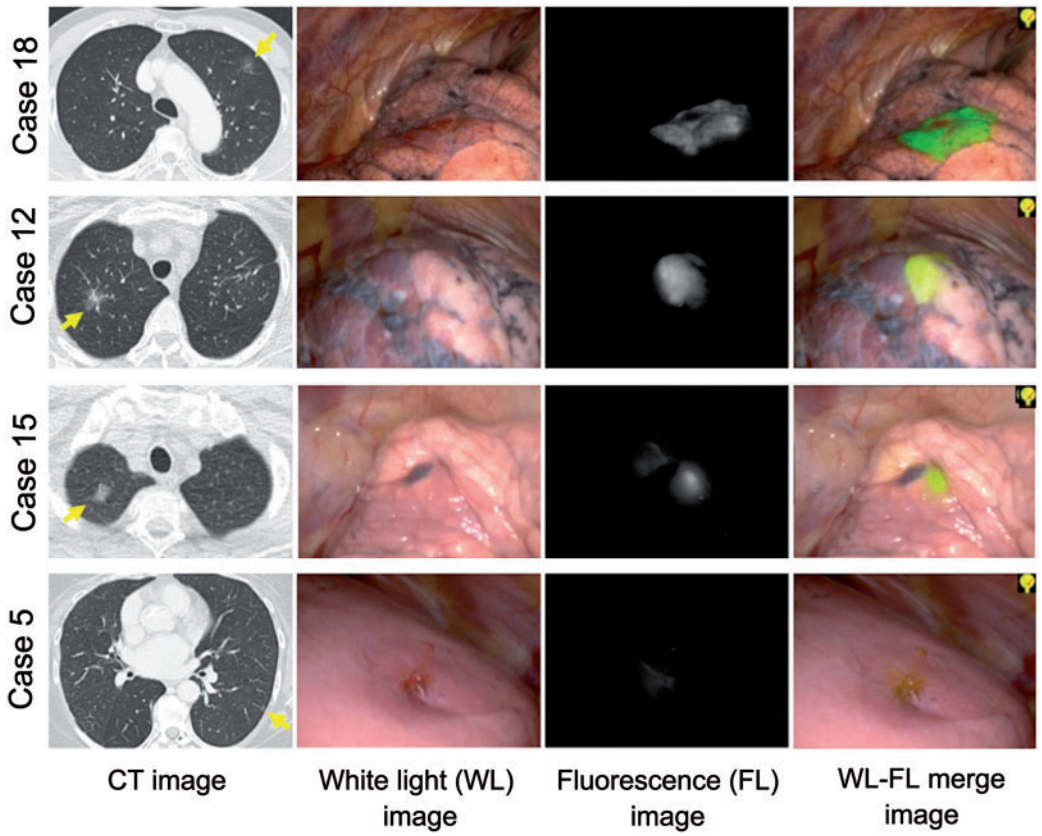

Figure 1: Multiple cases of intraoperative FL imaging used to detect lung nodules. Reproduced with permission from Elsevier, Ujiie *et al.* [53]. FL: fluorescence; WL: white light.

had a lung resection guided by IFI. In all 12 patients, the ICG 'tattoo' was identified and led to complete resection of the nodule. Nodules ranged in size from 0.4 cm to 2.1 cm with a depth from the pleural surface ranging from 0.4 to 2.0. As in other studies, these lesions represented solid, part-solid, mixed and pure ground-glass opacity lesions on CT. Ten of these patients had early lung cancers and underwent SLNB guided by ICG, which was successful in 80% of the patients. The 2 unsuccessful patients had technical issues with the delivery of the ICG. One of these 8 patients had a pathologically positive N2 SLN identified with IFI. The pathological status of all SLNs identified in this study reflected that of all nodes collected.

Two groups have shown that a systemically delivered dose of as low as 1 mg/kg of ICG given 24 h combined with IFI was able to detect 90% and 91% of pulmonary nodules respectively [56, 57]. IFI was used *in vivo* and *ex vivo*. The samples in 1 study were then sent for fluorescence microscopy to confirm the presence of ICG. These nodules ranged in size from 0.2 cm to 11 cm and were of a wide variety of malignant histologies, including primary lung cancers, carcinoid tumours, melanoma and metastatic pheochromocytomas. Both studies showed that the tumour depth from the pleural surface was a significant limitation to the ability of IFI to detect the nodule without transecting the parenchyma above the nodule. No major complications were attributed to the ICG or IFI. Singhal *et al.* [57–61] have also been able to detect a range of lung cancers, metastatic disease, visualize additional occult nodules at the time of surgery, locate sub-centimeter nodules and accurately visualize thymomas. It should be noted that ICG also accumulated in areas of inflammation, making it a sensitive but not specific contrast agent in these studies.

DIRECTIONS FOR THE FUTURE

IFI with ICG may have a number of practical applications within thoracic surgery. The studies already performed on SLNB, lung mapping, vascular assessment and nodule detection all show feasibility and potential promise in the clinical arena. There are also a few studies on other unique uses of ICG IFI in thoracic surgery such as for tracheal anastomosis and phrenic nerve identification [62, 63]. However, no high-level data identifying clear clinical applicability or benefit currently exist for IFI. Larger experiences and prospective trials will be needed to better delineate the indications and specific applications for IFI in thoracic surgical procedures.

As thoracic surgery moves towards more minimally invasive techniques, such as endoscopic and robotic procedures, there will be more need to enhance the surgeon's optical perception. These modalities, although potentially less traumatic to the patient, remove or distort haptic feedback to the surgeon [64, 65]. It may be anticipated that enhancement of visual feedback may become the primary means of interacting with the surgical field [66, 67].

The use of IFI in thoracic surgery may be expected to increase over the next several years. Contrast agent development is an active area of research and is by far the rate-limiting step of

advancing IFI technologies and capabilities. As an example, promising new folate-conjugated tracers have shown specificity for cancers with up-regulated folate receptors and may significantly increase the applicability of IFI in the detection and diagnosis of indeterminate pulmonary nodules [68, 69]. However, obtaining FDA approval for new tracers is an exhaustive process and can be expected to limit the clinical use of IFI in the immediate future. However, as new tracers and new techniques are developed, thoracic applications of IFI may help address some of the aforementioned challenges in thoracic surgical procedures. While it is not entirely clear what the full landscape of its utilization may be, it is not unreasonable to expect IFI will play an increasing role in the growing armamentarium of the thoracic surgeon.

ACKNOWLEDGEMENTS

The authors would like to acknowledge Madelaine Pisani for her contributions to this work.

Conflict of interest: none declared.

REFERENCES

[1] Solomon M, White BR, Nothdruft RE, Akers W, Sudlow G, Eggebrecht AT *et al*. Video-rate fluorescence diffuse optical tomography for in vivo sentinel lymph node imaging. Biomed Opt Express 2011;2:3267–77.
[2] Schols RM, Bouvy ND, van Dam RM, Masclee AAM, Dejong CHC, Stassen LPS. Combined vascular and biliary fluorescence imaging in laparoscopic cholecystectomy. Surg Endosc 2013;27:4511–7.
[3] van Dam GM, Themelis G, Crane LMA, Harlaar NJ, Pleijhuis RG, Kelder W *et al*. Intraoperative tumor-specific fluorescence imaging in ovarian cancer by folate receptor-α targeting: first in-human results. Nat Med 2011;17:1315–9.
[4] Can MF, Yagci G, Cetiner S. Systematic review of studies investigating sentinel node navigation surgery and lymphatic mapping for gastric cancer. J Laparoendosc Adv Surg Tech A 2013;23:651–62.
[5] Schaafsma BE, Verbeek FPR, Rietbergen DDD, van der Hiel B, van der Vorst JR, Liefers GJ *et al*. Clinical trial of combined radio- and fluorescence-guided sentinel lymph node biopsy in breast cancer. Br J Surg 2013;100:1037–44.
[6] Hirche C, Mohr Z, Kneif S, Doniga S, Murawa D, Strik M *et al*. Ultrastaging of colon cancer by sentinel node biopsy using fluorescence navigation with indocyanine green. Int J Colorectal Dis 2012;27:319–24.
[7] Gilmore DM, Khullar OV, Gioux S, Stockdale A, Frangioni JV, Colson YL *et al*. Effective low-dose escalation of indocyanine green for near-infrared fluorescent sentinel lymph node mapping in melanoma. Ann Surg Oncol 2013;20:2357–63.
[8] van der Vorst JR, Schaafsma BE, Hutteman M, Verbeek FPR, Liefers G-J, Hartgrink HH *et al*. Near-infrared fluorescence-guided resection of colorectal liver metastases. Cancer 2013;119:3411–8.
[9] Moody ED, Viskari PJ, Colyer CL. Non-covalent labeling of human serum albumin with indocyanine green: a study by capillary electrophoresis with diode laser-induced fluorescence detection. J Chromatogr B Biomed Sci Appl 1999;729:55–64.
[10] De Grand AM, Lomnes SJ, Lee DS, Pietrzykowski M, Ohnishi S, Morgan TG *et al*. Tissue-like phantoms for near-infrared fluorescence imaging system assessment and the training of surgeons. J Biomed Opt 2006;11:014007.
[11] Veronesi U, Paganelli G, Galimberti V, Viale G, Zurrida S, Bedoni M *et al*. Sentinel-node biopsy to avoid axillary dissection in breast cancer with clinically negative lymph-nodes. Lancet 1997;349:1864–7.
[12] Albertini JJ, Cruse CW, Rapaport D, Wells K, Ross M, DeConti R *et al*. Intraoperative radio-lympho-scintigraphy improves sentinel lymph node identification for patients with melanoma. Ann Surg 1996;223:217–24.
[13] Thompson JF, McCarthy WH, Bosch CMJ, O'Brien CJ, Quinn MJ, Paramaesvaran S *et al*. Sentinel lymph node status as an indicator of the presence of metastatic melanoma in regional lymph nodes. Melanoma Res 1995;5:255–60.
[14] Sonobe M, Yamada T, Sato M, Menju T, Aoyama A, Sato T *et al*. Identification of subsets of patients with favorable prognosis after recurrence in completely resected non-small cell lung cancer. Ann Surg Oncol 2014;21:2546–54.
[15] Nakagawa T, Okumura N, Ohata K, Igai H, Matsuoka T, Kameyama K. Postrecurrence survival in patients with stage I non-small cell lung cancer. Eur J Cardiothorac Surg 2008;34:499–504.
[16] Youlden DR, Cramb SM, Baade PD. The international epidemiology of lung cancer: geographical distribution and secular trends. J Thorac Oncol 2008;3:819–31.
[17] Little AG, Rusch VW, Bonner JA, Gaspar LE, Green MR, Webb WR *et al*. Patterns of surgical care of lung cancer patients. Ann Thorac Surg 2005;80:2051–6; discussion 2056.
[18] Wu N, Yan S, Lv C, Feng Y, Wang Y, Zhang L *et al*. Comparison of systematic mediastinal lymph node dissection versus systematic sampling for lung cancer staging and completeness of surgery. J Surg Res 2011;171:e169–73.
[19] Tiffet O, Nicholson AG, Khaddage A, Prévot N, Ladas G, Dubois F *et al*. Feasibility of the detection of the sentinel lymph node in peripheral non-small cell lung cancer with radio isotopic and blue dye techniques. Chest 2005;127:443–8.
[20] Schmidt FE, Woltering EA, Webb WR, Garcia OM, Cohen JE, Rozans MH. Sentinel nodal assessment in patients with carcinoma of the lung. Ann Thorac Surg 2002;74:870–5.
[21] Ito N, Fukuta M, Tokushima T, Nakai K, Ohgi S. Sentinel node navigation surgery using indocyanine green in patients with lung cancer. Surg Today 2004;34:581–5.
[22] Yamashita S-I, Tokuishi K, Miyawaki M, Anami K, Moroga T, Takeno S *et al*. Sentinel node navigation surgery by thoracoscopic fluorescence imaging system and molecular examination in non-small cell lung cancer. Ann Surg Oncol 2012;19:728–33.
[23] Yamashita S-I, Tokuishi K, Anami K, Miyawaki M, Moroga T, Kamei M *et al*. Video-assisted thoracoscopic indocyanine green fluorescence imaging system shows sentinel lymph nodes in non-small-cell lung cancer. J Thorac Cardiovasc Surg 2011;141:141–4.
[24] Gilmore DM, Khullar OV, Jaklitsch MT, Chirieac LR, Frangioni JV, Colson YL. Identification of metastatic nodal disease in a phase 1 dose-escalation trial of intraoperative sentinel lymph node mapping in non-small cell lung cancer using near-infrared imaging. J Thorac Cardiovasc Surg 2013;146:562–70; discussion 569–70.
[25] Nomori H, Cong Y, Sugimura H. Utility and pitfalls of sentinel node identification using indocyanine green during segmentectomy for cT1N0M0 non-small cell lung cancer. Surg Today 2016;46:908–13.
[26] Yuasa Y, Seike J, Yoshida T, Takechi H, Yamai H, Yamamoto Y *et al*. Sentinel lymph node biopsy using intraoperative indocyanine green fluorescence imaging navigated with preoperative CT lymphography for superficial esophageal cancer. Ann Surg Oncol 2012;19:486–93.
[27] Hachey KJ, Gilmore DM, Armstrong KW, Harris SE, Hornick JL, Colson YL *et al*. Safety and feasibility of near-infrared image-guided lymphatic mapping of regional lymph nodes in esophageal cancer. J Thorac Cardiovasc Surg 2016;152:546–54.
[28] Schlottmann F, Barbetta A, Mungo B, Lidor AO, Molena D. Identification of the lymphatic drainage pattern of esophageal cancer with near-infrared fluorescent imaging. J Laparoendosc Adv Surg Tech A 2017;27:268–71.
[29] Helminen O, Mrena J, Sihvo E. Near-infrared image-guided lymphatic mapping in minimally invasive oesophagectomy of distal oesophageal cancer. Eur J Cardiothorac Surg 2017; doi:10.1093/ejcts/ezx141.
[30] Landreneau RJ, Normolle DP, Christie NA, Awais O, Wizorek JJ, Abbas G *et al*. Recurrence and survival outcomes after anatomic segmentectomy versus lobectomy for clinical stage I non-small-cell lung cancer: a propensity-matched analysis. J Clin Oncol 2014;32:2449–55.
[31] Schuchert MJ, Abbas G, Pennathur A, Ferson PF, Wilson DO, Siegfried JM *et al*. Anatomic Lung Resection for Clinical Stage I Non-small Cell Lung Cancer (NSCLC): equivalent outcomes following anatomic segmentectomy and lobectomy. Chest 2010;138:758A–1–758A–2.
[32] Nomori H, Okada M. General Knack of Segmentectomy. Illustrated Anatomical Segmentectomy for Lung Cancer. Tokyo: Springer, 2012, 9–21.

[33] Oizumi H, Kato H, Endoh M, Inoue T, Watarai H, Sadahiro M. Techniques to define segmental anatomy during segmentectomy. Ann Cardiothorac Surg 2014;3:170–5.
[34] Misaki N, Chang SS, Igai H, Tarumi S, Gotoh M, Yokomise H. New clinically applicable method for visualizing adjacent lung segments using an infrared thoracoscopy system. J Thorac Cardiovasc Surg 2010;140:752–6.
[35] Kasai Y, Tarumi S, Chang SS, Misaki N, Gotoh M, Go T *et al*. Clinical trial of new methods for identifying lung intersegmental borders using infrared thoracoscopy with indocyanine green: comparative analysis of 2- and 1-wavelength methods. Eur J Cardiothorac Surg 2013;44:1103–7.
[36] Sekine Y, Ko E, Oishi H, Miwa M. A simple and effective technique for identification of intersegmental planes by infrared thoracoscopy after transbronchial injection of indocyanine green. J Thorac Cardiovasc Surg 2012;143:1330–5.
[37] Escofet X, Manjunath A, Twine C, Havard TJ, Clark GW, Lewis WG. Prevalence and outcome of esophagogastric anastomotic leak after esophagectomy in a UK regional cancer network. Dis Esophagus 2010; 23:112–6.
[38] Blewett CJ, Miller JD, Young JE, Bennett WF, Urschel JD. Anastomotic leaks after esophagectomy for esophageal cancer: a comparison of thoracic and cervical anastomoses. Ann Thorac Cardiovasc Surg 2001;7: 75–8.
[39] Alanezi K, Urschel JD. Mortality secondary to esophageal anastomotic leak. Ann Thorac Cardiovasc Surg 2004;10:71–5.
[40] Lee Y, Fujita H, Yamana H, Kakegawa T. Factors affecting leakage following esophageal anastomosis. Surg Today 1994;24:24–9.
[41] Linder G, Hedberg J, Björck M, Sundbom M. Perfusion of the gastric conduit during esophagectomy. Dis Esophagus 2016; doi:10.1111/dote.12537.
[42] Pham TH, Perry KA, Enestvedt CK, Gareau D, Dolan JP, Sheppard BC *et al*. Decreased conduit perfusion measured by spectroscopy is associated with anastomotic complications. Ann Thorac Surg 2011;91:380–5.
[43] Campbell C, Reames MK, Robinson M, Symanowski J, Salo JC. Conduit vascular evaluation is associated with reduction in anastomotic leak after esophagectomy. J Gastrointest Surg 2015;19:806–12.
[44] Miyazaki T, Kuwano H, Kato H, Yoshikawa M, Ojima H, Tsukada K. Predictive value of blood flow in the gastric tube in anastomotic insufficiency after thoracic esophagectomy. World J Surg 2002;26:1319–23.
[45] Kesler KA, Pillai ST, Birdas TJ, Rieger KM, Okereke IC, Ceppa D *et al*. 'Supercharged' isoperistaltic colon interposition for long-segment esophageal reconstruction. Ann Thorac Surg 2013;95:1162–8; discussion 1168–9.
[46] Varela E, Reavis KM, Hinojosa MW, Nguyen N. Laparoscopic gastric ischemic conditioning prior to esophagogastrectomy: technique and review. Surg Innov 2008;15:132–5.
[47] Kubota K, Yoshida M, Kuroda J, Okada A, Ohta K, Kitajima M. Application of the HyperEye Medical System for esophageal cancer surgery: a preliminary report. Surg Today 2013;43:215–20.
[48] Rino Y, Yukawa N, Sato T, Yamamoto N, Tamagawa H, Hasegawa S *et al*. Visualization of blood supply route to the reconstructed stomach by indocyanine green fluorescence imaging during esophagectomy. BMC Med Imaging 2014;14:18.
[49] Shimada Y, Okumura T, Nagata T, Sawada S, Matsui K, Hori R *et al*. Usefulness of blood supply visualization by indocyanine green fluorescence for reconstruction during esophagectomy. Esophagus 2011;8:259–66.
[50] Koyanagi K, Ozawa S, Oguma J, Kazuno A, Yamazaki Y, Ninomiya Y *et al*. Blood flow speed of the gastric conduit assessed by indocyanine green fluorescence: new predictive evaluation of anastomotic leakage after esophagectomy. Medicine (Baltimore) 2016;95:e4386.
[51] Blackmon SH, Feinglass SR. The United States preventive services task force recommendations for lung cancer screening. Thorac Surg Clin 2015;25:199–203.
[52] Cerfolio RJ, Bryant AS, McCarty TP, Minnich DJ. A prospective study to determine the incidence of non-imaged malignant pulmonary nodules in patients who undergo metastasectomy by thoracotomy with lung palpation. Ann Thorac Surg 2011;91:1696–700; discussion 1700–1.
[53] Ujiie H, Kato T, Hu H-P, Patel P, Wada H, Fujino K *et al*. A novel minimally invasive near-infrared thoracoscopic localization technique of small pulmonary nodules: a phase I feasibility trial. J Thorac Cardiovasc Surg 2017; doi:10.1016/j.jtcvs.2017.03.140.
[54] Abbas A, Kadakia S, Ambur V, Muro K, Kaiser L. Intraoperative electromagnetic navigational bronchoscopic localization of small, deep, or subsolid pulmonary nodules. J Thorac Cardiovasc Surg 2017;153:1581–90.
[55] Hachey KJ, Digesu CS, Armstrong KW, Gilmore DM, Khullar OV, Whang B *et al*. A novel technique for tumor localization and targeted lymphatic mapping in early-stage lung cancer. J Thorac Cardiovasc Surg 2017; doi: 10.1016/j.jtcvs.2016.12.058.
[56] Kim HK, Quan YH, Choi BH, Park J-H, Han KN, Choi Y *et al*. Intraoperative pulmonary neoplasm identification using near-infrared fluorescence imaging. Eur J Cardiothorac Surg 2016;49:1497–502.
[57] Okusanya OT, Holt D, Heitjan D, Deshpande C, Venegas O, Jiang J *et al*. Intraoperative near-infrared imaging can identify pulmonary nodules. Ann Thorac Surg 2014;98:1223–30.
[58] Keating J, Newton A, Venegas O, Nims S, Zeh R, Predina J *et al*. Near-infrared intraoperative molecular imaging can locate metastases to the lung. Ann Thorac Surg 2016; doi:10.1016/j.athoracsur.2016.08.079.
[59] Keating J, Judy R, Newton A, Singhal S. Near-infrared operating lamp for intraoperative molecular imaging of a mediastinal tumor. BMC Med Imaging 2016;16:15.
[60] Keating JJ, Kennedy GT, Singhal S. Identification of a subcentimeter pulmonary adenocarcinoma using intraoperative near-infrared imaging during video-assisted thoracoscopic surgery. J Thorac Cardiovasc Surg 2015;149:e51–3.
[61] Keating J, Singhal S. Novel methods of intraoperative localization and margin assessment of pulmonary nodules. Semin Thorac Cardiovasc Surg 2016;28:127–36.
[62] Wagner OJ, Louie BE, Vallières E, Aye RW, Farivar AS. Near-infrared fluorescence imaging can help identify the contralateral phrenic nerve during robotic thymectomy. Ann Thorac Surg 2012;94:622–5.
[63] Schweiger T, Schwarz S, Traxler D, Dodier P, Aigner C, Lang G *et al*. Bronchoscopic indocyanine green fluorescence imaging of the anastomotic perfusion after tracheal surgery. Ann Thorac Surg 2016;101: 1943–9.
[64] Bethea BT, Okamura AM, Kitagawa M, Fitton TP, Cattaneo SM, Gott VL *et al*. Application of haptic feedback to robotic surgery. J Laparoendosc Adv Surg Tech A 2004;14:191–5.
[65] Tholey G, Desai JP, Castellanos AE. Force feedback plays a significant role in minimally invasive surgery: results and analysis. Ann Surg 2005; 241:102–9.
[66] Hagen ME, Meehan JJ, Inan I, Morel P. Visual clues act as a substitute for haptic feedback in robotic surgery. Surg Endosc 2008;22:1505–8.
[67] Kitagawa M, Dokko D, Okamura AM, Yuh DD. Effect of sensory substitution on suture-manipulation forces for robotic surgical systems. J Thorac Cardiovasc Surg 2005;129:151–8.
[68] Okusanya OT, DeJesus EM, Jiang JX, Judy RP, Venegas OG, Deshpande CG *et al*. Intraoperative molecular imaging can identify lung adenocarcinomas during pulmonary resection. J Thorac Cardiovasc Surg 2015; 150:28–35.e1.
[69] Keating JJ, Okusanya OT, De Jesus E, Judy R, Jiang J, Deshpande C *et al*. Intraoperative molecular imaging of lung adenocarcinoma can identify residual tumor cells at the surgical margins. Mol Imaging Biol 2016;18: 209–18.